A Comparative Small Signal Stability Analysis of PMSG and SCIG-Based Wind Farms

H. Ahmadi, H. Ghasemi and H. Lesani
University of Tehran, School of Electrical and Computer Engineering, Tehran, Iran

Keywords: Inter-Area Mode, Local Mode, PMSG, SCIG

Abstract:
The increasing interest in exploiting renewable energy resources has introduced a new generation of energy conversion technologies including wind farms (WF) to the power systems. Previous studies of these WFs and their impacts on power systems have made new challenges emerge, which in turn, require detailed assessment for continuously increasing wind power penetration. Among these challenges, the power system transients and its small signal stability are from crucial importance. In this paper, the small signal stability assessment of increasing output power of WFs with fixed installed capacity is carried out. For a fixed capacity, the variations of wind speed leads to different levels of power injections from WFs, thus, considering the dispatching operation and unit commitment, leading to changes in power obtained from conventional synchronous machine-based plants. Permanent magnet synchronous generator (PMSG) and squirrel cage induction generator (SCIG)-based WFs are studied and compared. The results have shown that the impact of injected power from WFs on power system oscillations depends on several factors including wind speed, WF location in power system and the employed control strategies in WFs. Furthermore, it is shown that the contribution of the PMSG-based WFs on the oscillation damping is more effective than that of the SCIG-based one.

I. INTRODUCTION

A rate of rise about 25% per year of installed wind power generation capacity has been reported worldwide [1]. Compared to the other renewable energy resources such as solar, geothermal and etc., wind energy has received more attention with higher growth. The remarkable advancements which have been reached during the past decade in wind power generation technology along with the environmental issues pertaining to the fuel-consuming power plants have made the wind power one of the most economical resources for replacing the conventional power plants.
Wind power integration, in turn, will introduce new issues to the existing power systems from several aspects, especially when the level of penetration is significant. Among these aspects, the system stability is from crucial importance. Conventional generators are

generally synchronous machines with high inertia, coupled to the steam or hydro turbines. The reciprocal effects of these types of machines were broadly studied in detail and concepts such as inter and intra-area (local) oscillations have been defined [2]. Since the nature of the wind turbine generators (WTG) is basically different from the synchronous generators due to the power electronic interfaces and induction generators application, the well-known stability problems have to be investigated.

Several types of WTGs are commercially available today including: squirrel cage induction generators (SCIG), doubly-fed induction generators (DFIG) and direct drive synchronous generators (DDSG) or permanent magnet synchronous generators (PMSG).Two more general categories are fixed-speed and variable speed generators [3].

Some research work has been conducted to study the stability issues corresponding to the WFs. In [4], an approach for sensitivity analysis of electromechanical modes (EMM) to the inertia of the generators is introduced and the results have shown both detrimental and beneficial impacts of increased DFIG penetration into the power system. Inter-area and local oscillations have been investigated in [5] in a benchmark test system. The results are reported for both the variable and fixed-speed turbines replacing the conventional generation units. It is shown that the damping of EMMs is improved as the level of penetration is increased. However, in the case of large amounts of installed WFs, there is a possibility for the inter-area modes to be adversely affected.

Different control strategies for DFIGs and their impacts on the system stability were investigated in [6]. The SCIGs have been shown to increase the eigenvalues damping.

Different control strategies for PMSGs and their impacts on power system performance were investigated in [7]. Maximum power point tracking and maximum efficiency controls of PMSGs are also studied in [8].

A comparison between the DFIGs and PMSGs for small signal stability behavior is carried out in [9]. It is shown that the PMSGs are more powerful to damp the oscillations in power system. The transient stability margins in terms of critical clearing time (CCT) are demonstrated to be higher for PMSG-based WFs in comparison to DFIG-based WFs [9]. Proposed designs of synchronous machine for wind turbine application in order to reduce the oscillations are available in the literature [10]. With such a design, the gearbox is not necessary anymore and the generator can be directly driven by the turbine, as is the case for DDSG. However, modal analysis is not performed to investigate the stability issues of PMSG-based WFs in previous literatures.

The effects of the system parameters in a power system including fixed-speed WTGs on the transient stability are studied in [11]. The increasing in the generator slip is recognized to be responsible for the instability of fixed-speed WTGs.

There are a few documents about the eigenvalue analysis of the PMSG-based WFs for stability assessment. Besides, comparative studies on the impacts of SCIGs and PMSGs on power system small signal stability have not yet been performed. In this paper, we have carried out this analysis in MATLAB/PSAT.

This paper is organized as follows. Section II describes the modeling procedure of different WTG in MATLAB/PSAT. Section III explains the two-area test system used in this study. Achieved results along with a brief discussion are reported in Section IV. Eventually, the paper concludes with a summary of the main achievements of this paper.

II. WTG MODELING PROCEDURE

A general block diagram of an induction machine (IM) based WTG is shown in Fig. 1. It consists of the blades, rotor shaft, gearbox, the induction generator and the interface with the network. The blades and gearbox with the relating pitch-angle controller are modeled as a wind turbine, which converts the wind energy into the mechanical torque applied to the induction generator. The output power of this turbine is given by [12]

$$P_{out} = c_p(\lambda,\beta)\frac{\rho A}{2}v_w^3 \quad (1)$$

where P_{out} is the mechanical output power of the turbine (W), c_p is the performance coefficient of the turbine, ρ is the air density (kg/m^3), A is the turbine swap area (m^2), v_w is the wind speed (m/s), λ is the ratio of the rotor blade tip speed to wind speed and β is the blade pitch angle (deg). c_p is related to λ and β as

$$c_p(\lambda,\beta) = c_1\left(\frac{c_2}{\lambda_i} - c_3\beta - c_4\right)e^{\frac{c_5}{\lambda_i}} + c_6\lambda\,,$$
$$\frac{1}{\lambda_i} = \frac{1}{\lambda - 0.08\beta} - \frac{0.035}{\beta^3+1} \quad (2)$$

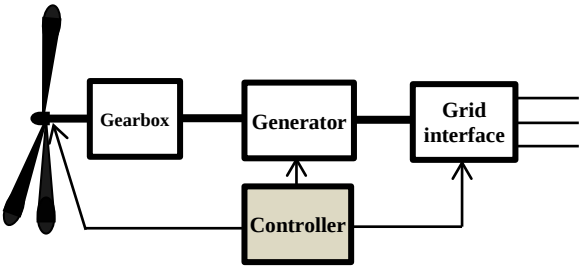

Fig. 1. General overview of a WTG

Values of the parameters c_1 to c_6 are given in [13]. A typical turbine speed–output power characteristic, which is used in this study, is given in Fig. 2. Points A, B, C and D are given in Appendix. The reference power is determined by the tracking characteristic of the wind turbine (points A, B, C and D in Fig. 2). This wind turbine is used for all studies.

A. Modeling of the Induction Machine

The asynchronous machine model is obtained from [13]. A fourth-order model is used for the electrical part with equivalent circuit shown in Fig. 3.The state-space equations in d-q frame are as follows:

$$\begin{aligned} V_{qs} &= R_s i_{qs} + \frac{d\varphi_{qs}}{dt} + \omega\varphi_{ds} \\ V_{ds} &= R_s i_{ds} + \frac{d\varphi_{ds}}{dt} - \omega\varphi_{qs} \\ V'_{qr} &= R'_r i'_{qr} + \frac{d\varphi'_{qr}}{dt} + (\omega-\omega_r)\varphi'_{dr} \\ V'_{dr} &= R'_r i'_{dr} + \frac{d\varphi'_{dr}}{dt} - (\omega-\omega_r)\varphi'_{qr} \end{aligned} \quad (3)$$

$$T_e = \frac{3}{2}p\left(\varphi_{ds}i_{qs} - \varphi_{qs}i_{ds}\right) \quad (4)$$

where

$$\begin{aligned} \varphi_{ds} &= L_s i_{qs} + L_m i'_{qr} \\ \varphi_{qs} &= L_s i_{ds} + L_m i'_{dr} \\ \varphi'_{qr} &= L'_r i'_{qr} + L_m i_{qs} \\ \varphi'_{dr} &= L'_r i'_{dr} + L_m i_{ds} \\ L_s &= L_{ls} + L_m \\ L'_r &= L'_{lr} + L_m \end{aligned} \quad (5)$$

The mechanical part is described as a two-mass model:

$$\begin{aligned} \frac{d\omega_{wr}}{dt} &= \frac{T_{wr} - K_s\gamma}{2H_{wr}} \\ \frac{d\omega_m}{dt} &= \frac{K_s\gamma - T_e}{2H_m} \\ \frac{d\gamma}{dt} &= 2\pi f(\omega_{wr} - \omega_m) \end{aligned} \quad (6)$$

where f is the nominal grid frequency (Hz), T_e is the electrical generated torque (p.u.), γ is the angular displacement between the two ends of the shaft (electrical radians), ω_{wr} is the rotational speed of wind turbine rotor (p.u.), ω_m is the rotational speed of the generator (p.u.), H is the inertia constant (s) and K_s is the shaft stiffness (p.u. torque/electrical radians).

B. Modeling of the PMSG

Figure 4 displays the general form of the PMSG-based WTG. The converter includes two parts namely the machine-side converter (MSC) and the grid-side converter (GSC).

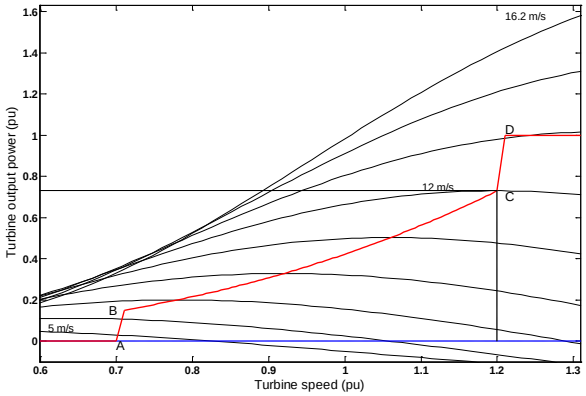

Fig. 2. A typical characteristic of turbine speed–output power of a WTG for different wind speeds.

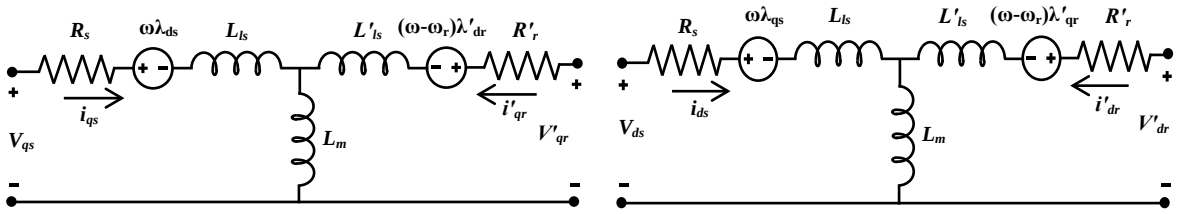

Fig. 3. Equivalent d-q circuits for the induction machine. The subscripts *s* and *r* refer to the stator and rotor side parameters, respectively.

The converter controllers give the ability to set the frequency and magnitude of the injected voltage to the grid. Because the generator is fully decoupled from the network, the generated reactive power Q_s is absorbed by MSC and the amount of injected reactive power to the grid is determined by GSC and not the generator itself.

State-space equations for the PMSG in d-q reference frame are given as following [3]

$$\begin{gathered} v_{ds} = -R_s i_{ds} + \omega_m \left(L_{s\sigma} + L_{qm}\right) i_{qs} \\ v_{qs} = \\ -R_s i_{qs} - \omega_m \left[\left(L_{s\sigma} + L_{qm}\right) i_{ds} - \varphi_p\right] \\ P_s = v_{ds} i_{ds} + v_{qs} i_{qs} \\ Q_s = v_{qs} i_{ds} - v_{ds} i_{qs} \end{gathered} \tag{7}$$

The injected active and reactive powers to the grid from GSC are

$$\begin{aligned} P_c &= v_{dc} i_{dc} + v_{qc} i_{qc} \\ Q_c &= v_{qc} i_{dc} - v_{ds} i_{qs} \end{aligned} \tag{8}$$

The converter voltage is a function of the grid voltage phase and magnitude as

$$\begin{aligned} v_{dc} &= V sin(-\theta) \\ v_{qc} &= V cos(\theta) \end{aligned} \tag{9}$$

The reactive power injected by GSC is then

$$Q_c = \frac{1}{\cos(\theta)} V\, i_{dc} + \tan(\theta) P_s \tag{10}$$

The mechanical equations for a single shaft model are

$$\begin{aligned} \dot{\omega}_m &= \frac{1}{2H_m}(T_m - T_e) \\ \dot{\theta}_m &= \omega_m \\ T_e &= \psi_{ds} i_{qs} - \psi_{qs} i_{ds} \end{aligned} \tag{11}$$

Stator fluxes and generator currents are linked as

$$\begin{aligned} \psi_{ds} &= -x_d i_{ds} + \psi_p \\ \psi_{qs} &= -x_q i_{qs} \end{aligned} \tag{12}$$

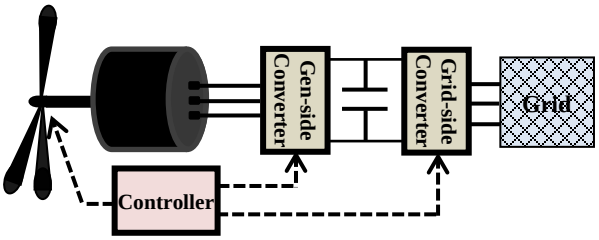

Fig. 4. General representation of a PMSG-based WTG

Due to the comparatively fast nature of the converter dynamics, a simple model as ideal current sources is assumed for the converter where i_{qs}, i_{ds} and i_{dc} are used for rotor speed control and the reactive power control, and the voltage control respectively. For these currents we have

$$\begin{aligned} \frac{di_{qs}}{dt} &= \frac{i_{qs\_ref} - i_{qs}}{T_{ep}} \\ \frac{di_{ds}}{dt} &= \frac{i_{ds\_ref} - i_{ds}}{T_{eq}} \\ \frac{di_{dc}}{dt} &= \frac{K_V\left(V_{ref} - V\right) - i_{dc}}{T_V} \end{aligned} \tag{13}$$

where

$$i_{qs_{ref}} = \frac{P_\omega^*(\omega_m)}{\omega_m \psi_{ds}} \tag{14}$$

$$i_{ds\_ref} = \frac{\psi_p}{x_d} - \sqrt{\left(\frac{\psi_p}{x_d}\right)^2 - \frac{Q_{ref}}{\omega_m x_d}}$$

$P_\omega^*(\omega_m)$ in Eq. 14 is obtained from the tracking characteristics in Fig. 2.

The time constants of pitch angle controller are large compared to power system transients period and the wind speed is kept between the allowable values. Therefore this controller is not used here.

III. TEST SYSTEM DESCRIPTION

The two-area four-machine system is used in simulation studies in this work [2]. This network is portrayed in Fig. 5. G1 and G2 are in Area 1 and G3 and G4 are in Area 2. Generators in the same area may oscillate against each other or against generators in the other area. These characteristics are referred to as the intra and inter-area oscillations, respectively.

In order to include the WF in the system, a WF is connected to Bus6 through a transformer. For simplicity, the aggregated model of small wind turbines is used here which does not affect the results [14], [15]. As the speed of the wind increases and so does the generated power by the WF, the output power of G2 is decreased, accordingly. This is done to utilize the maximum available power from the WFs and lower the generated power by the expensive conventional power plants. The WF consists of 600 1.5MW WTGs and corresponding data for each generator is given in Appendix. The governors of the steam power plants are not modeled and only the AVRs are considered. An eighth-order model for the synchronous generators including the sixth-order electrical model and second-order mechanical model is employed here, as described in [2].

IV. RESULTS AND DISCUSSION

A comparative study is done for the two different WTGs described in Section II in order to investigate their effects on the EMMs of power system. Eight cases are assumed in which the WF output power is increased by steps of 100MW.

In the first study, an aggregated model of the PMSG-based WF with the installed capacity of 900MW, the same as G2, is assumed. Table I represents the participation factors (PF) and damping ratios (DR) for each eigenvalue. The corresponding eigenvalue trajectories are shown in Fig. 7. The following equation is used for calculating the DR of an eigenvalue of the form $e = \alpha \pm j\omega$:

$$DR = \frac{-\alpha}{\sqrt{\alpha^2 + \omega^2}} \quad (15)$$

The eigenvalues are recognized considering the corresponding PFs and mode shapes. For better understanding, the PFs and mode shapes for Case 5 in Table 1 are given in Figs. 6 and 9, respectively.

In the second study, SCIG replaces PMSG. PFs and DRs for the eight cases in this part of the study are reported in Table II. Figure 8 depicts the corresponding eigenvalue trajectories.

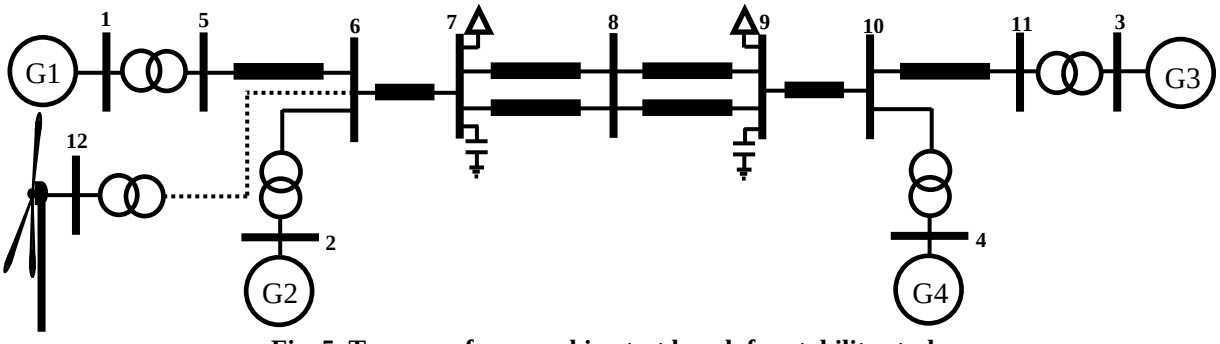

Fig. 5. Two-area four-machine test bench for stability study

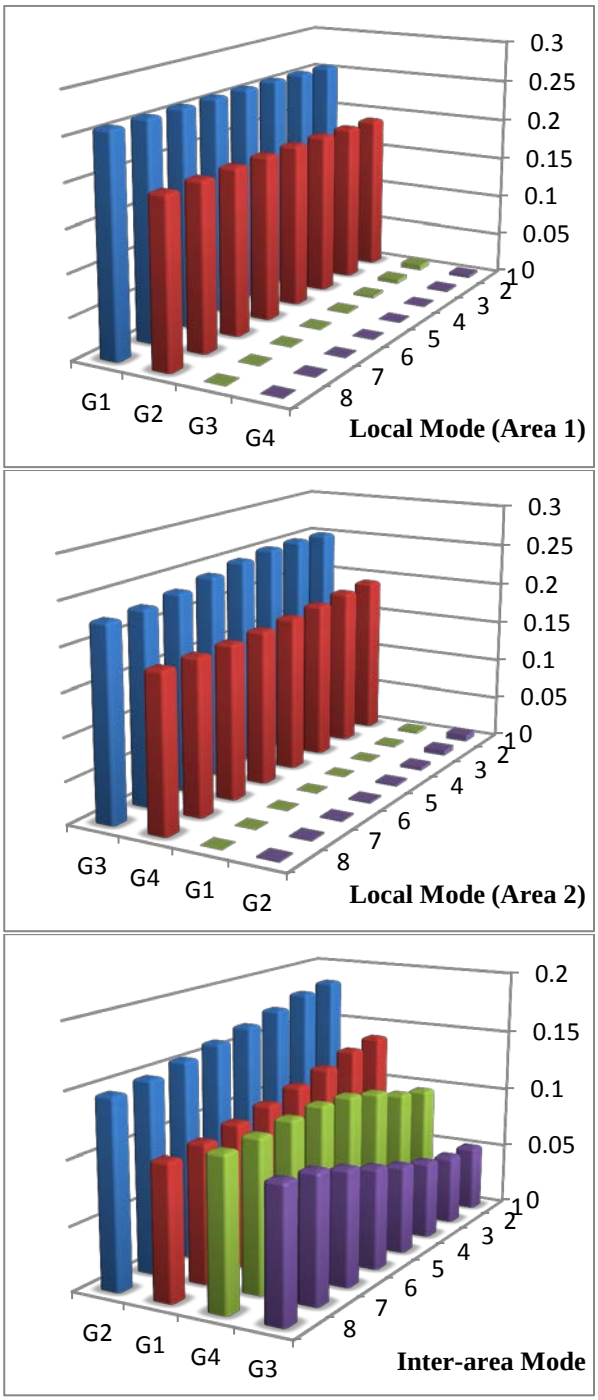

Fig. 6. Participation factors corresponding to the eigenvalue magnified in Fig. 7.

As it can be seen in Figs. 7 and 8, the local mode in Area 1 becomes more stable since by increasing WF output power, G2's output decreases. On the other hand, note that the local mode in Area 2 does not move as much as local mode in Area 1. Extra damping observed for local mode in Area 1 can be further enhanced by means of using new control strategies [7], [8].

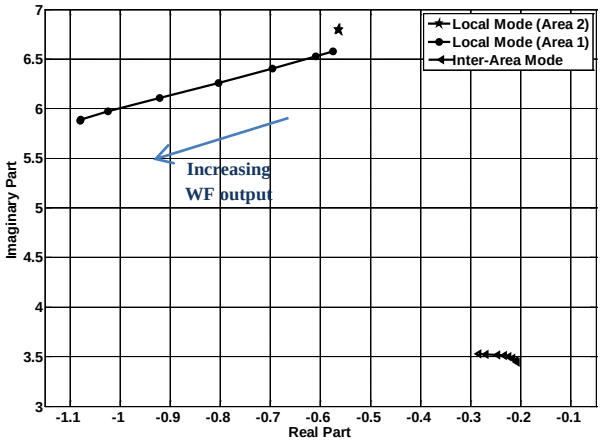

Fig. 7. Variation of the EMMs in the presence of PMSG-based WF.

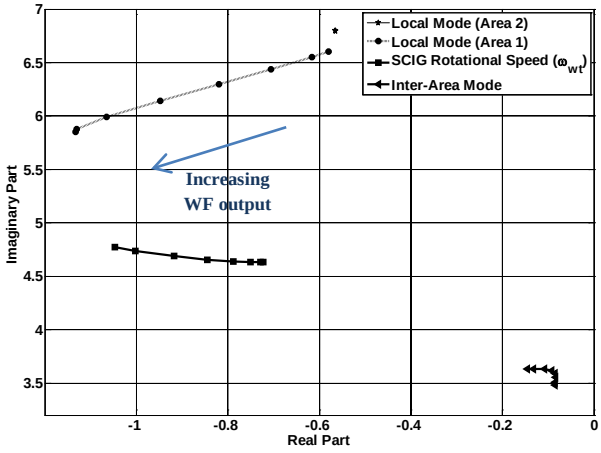

Fig. 8. Variation of the EMMs in the presence of SCIG-based WF.

Comparing the PMSG and SCIG-based WFs from the viewpoint of small signal stability, the latter is more powerful in damping the inter-area oscillations. Although the SCIGs were employed before due to their simple structure, the increasing interest in installing large scale WFs requires more controllable technologies such as PMSGs and DFIGs.

V. CONCLUSIONS

Modeling procedure of SCIGs and PMSGs are reviewed. WFs based on SCIGs and PMSGs from the viewpoint of small signal stability are investigated and compared. A fixed installed capacity for WFs is assumed and wind speed is increased stepwise. The trajectory of inter-area and local modes for increasing steps of WF's output power in the two-area test system are obtained and the corresponding PFs and DRs

for are reported. The PMSG-based WFs, when compared to the SCIG-based WFs, is shown to be more effective in damping the inter-area oscillations. However, not much difference was observed in the impacts of these two technologies on local modes. It is concluded that the impacts of increasing the WF output power on the small signal stability are beneficial. These impacts are dependent on the level of WF output power and the technology that is employed for energy conversion.

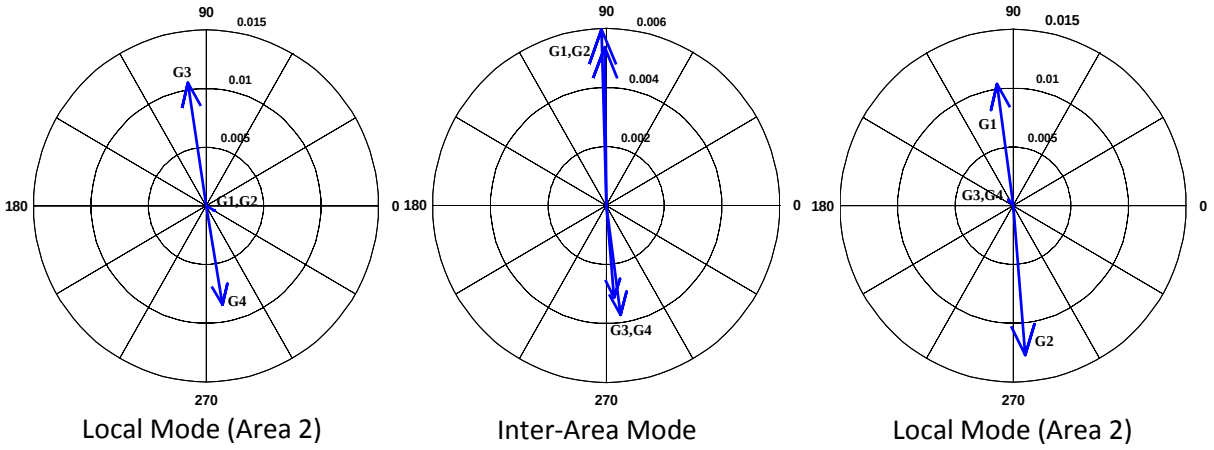

Fig. 9. Mode shapes for Case 5 in Table 1 corresponding to EMMs.

TABLE I
PFs corresponding to the EMMs for eight cases of increasing the PMSG-based WF output power.

	EEMs	PF of G1	PF of G2	PF of G3	PF of G4	I_{dc} PMSG	Frequency (Hz)	Damping ratio
Case1 ($P_{wind\ farm}$=10MW)	-0.5651±j6.7979	0.2565	0.1914	0.0066	0.0035	0	1.0819	0.0828
	-0.5753±j6.5799	0.0029	0.0082	0.2513	0.1937	0.0002	1.0472	0.0871
	-0.2076±j3.4474	0.1346	0.1820	0.0424	0.0685	0.0104	0.5486	0.0601
Case2 ($P_{wind\ farm}$=100MW)	-0.5651±j6.7976	0.2577	0.1932	0.0049	0.0023	0	1.0819	0.0828
	-0.6096±j6.5285	0.0017	0.0063	0.2530	0.1922	0.0003	1.0436	0.0930
	-0.2105±j3.4595	0.1334	0.1809	0.0435	0.0700	0.0091	0.5505	0.0607
Case3 ($P_{wind\ farm}$=200MW)	-0.5647±j6.7967	0.2590	0.1955	0.0027	0.0009	0	1.0817	0.0828
	-0.6957±j6.4050	0.0005	0.0038	0.2529	0.1889	0.0005	1.0194	0.0108
	-0.2174±j3.4820	0.1307	0.1784	0.0468	0.0723	0.0067	0.5542	0.0623
Case4 ($P_{wind\ farm}$=300MW)	-0.5642±j6.7958	0.2593	0.1968	0.0015	0.0004	0	1.0816	0.0827
	-0.8031±j6.2593	0	0.0024	0.2487	0.1861	0.0006	0.9962	0.1273
	-0.2249±j3.5011	0.1279	0.1759	0.0519	0.0737	0.0045	0.5572	0.0641
Case5 ($P_{wind\ farm}$=400MW)	-0.5637±j6.7947	0.2594	0.1976	0.0009	0.0003	0	1.0814	0.0827
	-0.9207±j6.1069	0	0.0018	0.2419	0.1842	0.0007	0.9719	0.1491
	-0.2335±j3.5141	0.1254	0.1736	0.0587	0.0739	0.0028	0.5593	0.0663
Case6 ($P_{wind\ farm}$=500MW)	-0.5633±j6.7935	0.2593	0.1980	0.0006	0.0002	0	1.0812	0.0826
	-1.0238±j5.9738	0	0.0016	0.2347	0.1834	0.0007	0.9507	0.1689
	-0.2471±j3.5195	0.1233	0.1715	0.0665	0.0732	0.0015	0.5601	0.0700
Case7 ($P_{wind\ farm}$=600MW)	-0.5629±j6.7920	0.2593	0.1983	0.0005	0.0002	0	1.081	0.0826
	-1.0785±j5.8921	0.0002	0.0017	0.2295	0.1840	0.0006	0.9377	0.1796
	-0.2700±j3.5225	0.1209	0.1688	0.0742	0.0732	0.0009	0.5606	0.0365
Case8 ($P_{wind\ farm}$=700MW)	-0.5628±j6.7912	0.2592	0.1983	0.0004	0.0002	0	1.0808	0.0826
	-1.0798±j5.8786	0.0003	0.0017	0.2281	0.1851	0.0005	0.9356	0.1807
	-0.2842±j3.5270	0.1193	0.1669	0.0779	0.0741	0.0009	0.5613	0.0803

TABLE II
PFs corresponding to the EMMs for eight cases of increasing the SCIG-based WF output power.

	EMMs	PF of G1	PF of G2	PF of G3	PF of G4	ω_{wt} SCIG	Frequency (Hz)	Damping ratio
Case1 ($P_{wind\ farm}$=10MW)	-0.5661±j6.7994	0.2576	0.1919	0.0060	0.0024	0	1.0822	0.0830
	-0.5805±j6.6014	0.0023	0.0067	0.2541	0.1895	0.0019	1.0506	0.0876
	-0.7223±j4.6334	0.0020	0.0024	0.0313	0.0681	0.3821	0.7374	0.1540
	-0.0854±j3.4822	0.1395	0.1848	0.0526	0.0973	0.0408	0.5542	0.0245
Case2 ($P_{wind\ farm}$=100MW)	-0.5659±j6.7989	0.2587	0.1937	0.0042	0.0014	0	1.0821	0.0829
	-0.6162±j6.5533	0.0012	0.0048	0.2550	0.1889	0.0019	1.0430	0.0936
	-0.7284±j4.6336	0.0021	0.0026	0.0325	0.0673	0.3820	0.7374	0.1553
	-0.0847±j3.5076	0.1360	0.1811	0.0556	0.1033	0.0405	0.5584	0.0241
Case3 ($P_{wind\ farm}$=200MW)	-0.5654±j6.7980	0.2597	0.1959	0.0021	0.0004	0	1.0819	0.0829
	-0.7062±j6.4367	0.0003	0.0026	0.2533	0.1867	0.0019	1.0244	0.1091
	-0.7506±j4.6353	0.0021	0.0031	0.0357	0.0639	0.3809	0.7377	0.1598
	-0.0840±j3.5540	0.1292	0.1739	0.0624	0.1135	0.0396	0.5656	0.0236
Case4 ($P_{wind\ farm}$=300MW)	-0.5649±j6.7972	0.2599	0.1969	0.0011	0.0002	0	1.0818	0.0828
	-0.8201±j6.2957	0	0.0016	0.2480	0.1836	0.0025	1.0020	0.1292
	-0.7886±j4.6409	0.0021	0.0035	0.0404	0.0581	0.3789	0.7386	0.1675
	-0.0855±j3.5921	0.1230	0.1673	0.0706	0.1203	0.0377	0.5716	0.0238
Case5 ($P_{wind\ farm}$=400MW)	-0.5646±j6.7962	0.2599	0.1974	0.0006	0.0001	0	1.0817	0.0828
	-0.9482±j6.1401	0	0.0011	0.2404	0.1792	0.0043	0.9772	0.1526
	-0.8446±j4.6562	0.0020	0.0037	0.0470	0.0507	0.3745	0.7410	0.1785
	-0.0925±j3.6185	0.1176	0.1614	0.0803	0.1229	0.0343	0.5759	0.0256
Case6 ($P_{wind\ farm}$=500MW)	-0.5644±j6.7951	0.2599	0.1977	0.0004	0.0001	0	1.0815	0.0828
	-1.0650±j5.9905	0.0001	0.0009	0.2325	0.1732	0.0079	0.9534	0.1750
	-0.9174±j4.6882	0.0015	0.0036	0.0554	0.0438	0.3648	0.7461	0.1920
	-0.1084±j3.6316	0.1128	0.1558	0.0908	0.1218	0.0291	0.5779	0.0298
Case7 ($P_{wind\ farm}$=600MW)	-0.5644±j6.7939	0.2598	0.1978	0.0003	0.0001	0	1.0813	0.0828
	-1.1305±j5.8790	0.0002	0.0009	0.2266	0.1677	0.0125	0.9356	0.1888
	-1.0023±j4.7394	0.0011	0.0033	0.0649	0.0383	0.3493	0.7543	0.2069
	-0.1327±j3.6336	0.1083	0.1501	0.1007	0.1192	0.0224	0.5783	0.0365
Case8 ($P_{wind\ farm}$=700MW)	-0.5645±j6.7932	0.2598	0.1978	0.0003	0.0001	0	1.0812	0.0828
	-1.1331±j5.8494	0.0002	0.0010	0.2248	0.1666	0.0145	0.9309	0.1902
	-1.0469±j4.7714	0.0009	0.0031	0.0690	0.0352	0.3404	0.7593	0.2143
	-0.1453±j3.6324	0.1062	0.1472	0.1052	0.1183	0.0186	0.5781	0.0400

REFERENCES

[1] Wind Power Monthly (1999) 15(5).

[2] P. Kundur, Power System Stability and Control, McGraw-Hill, 1994.

[3] T. Ackerman, Wind Power in Power Systems, Wiley, 2005

[4] D. Guatam, V. Vittal, T. Harbour, Impact of Increased Penetration of DFIG-Based Wind Turbine Generators on Transient and Small Signal Stability of Power Systems, IEEE Trans. Power Syst., 24 (3) (2009) 1426-1434.

[5] J J.G. Slootweg, W.L. Kling, The impact of large scale wind power generation on power system oscillations, Electr. Power Syst. Res. 67 (1) (2003) 9–20.

[6] R.D. Fernandez, R.J. Mantz, P.E. Battaiotto, Impact of wind farms on a power system: An eigenvalue analysis approach, Renew. Energy 32 (10) (2007) 1676–1688.

[7] S. Li, T. A. Haskew, L. Xu, Conventional and novel control designs for direct driven PMSG wind turbines, Elec. Power syst. Res. 80 (3) (2010) 328-338.

[8] M. Chinchilla, S. Arnaltes, J.C. Burgos, Control of permanent-magnet generator applied to variable-speed wind-energy systems connected to grid, IEEE Trans. Energy Conver. 21 (1) (2006) 130–135.

[9] F. Wu, X.-P. Zhang, P. Ju, Small signal stability analysis and control of the wind turbine with the direct-drive permanent magnet generator integrated to the grid, Elec. Power Syst. Res. 79 (2009) 1661-1667.

[10] A.J.G. Westlake, J.R. Bumby, E. Spooner, Damping the power-angle oscillations of a permanent-magnet synchronous generator with particular reference to wind turbine application, IEE Proc. Electr. Power Appl. 143 (3) (1996) 269–280.

[11] M. Rahimi, M. Parniani, Dynamic behavior and transient stability analysis of fixed speed wind turbines, Renew. Energy 34 (2009) 2613–2624.

[12] Siegfried Heier, "Grid Integration of Wind Energy Conversion Systems," John Wiley & Sons Ltd, 1998
[13] Krause, P.C., O. Wasynczuk, and S.D. Sudhoff, Analysis of Electric Machinery, IEEE Press, 2002.
[14] L.M. Fernández, C.A. García, J.R. Saenz, F. Jurado, Equivalent models of wind farms by using aggregated wind turbines and equivalent winds, Energy Conv. Man. 50 (3) (2009) 691-704.
[15] J. Conroy, R. Watson, Aggregate modeling of wind farms containing full-converter wind turbine generators with permanent magnet synchronous machines: transient stability studies, IET Renew. Power Gener. 3 (1) (2009) 39-52.

APPENDIX

Induction Machine

Power	Voltage	Frequency	X_d	X_q	ψ_p	X'_{lr}	H_m	P
1.5 MW	575V	60Hz	1	0.8	1	0.08	3	4

PMSG

Power	Voltage	Frequency	R_s	X_{ls}	R'_r	X'_{lr}	X_m	H_g	H_t	F	P	Voltage controller gain and time constant [K_V, T_V]	Active and reactive power control time constants [T_{ep} , T_{eq}]
1.5 MW	575V	60Hz	0.01	0.1	0.01	0.08	3	0.8	2.5	0.01	4	[10 , 1]	[0.01 0.01]

Turbine Data

Rated Power	Speeds at A,B,C,D	Power at C	Wind speed at C
1.5MW	0.7,0.71,1.2,1.21	0.73	15m/s